Clinical and experimental investigation of bone replacement

PhD Thesis

Dr. Krisztián Szalay

Semmelweis University
Doctoral School of Clinical Medicine

Thesis supervisor: Dr. Miklós Szendrői, DSc

Official opponents: Dr. Gergely Pánics, Ph.D.
Dr. István Böröcz, Ph.D.

Head of the PhD Examination Committee:
Dr. Péter Lakatos, DSc

Members of the Doctoral Examination Committee:
Dr. Károly Pap, Ph.D.
Dr. Tamás Klára, Ph.D.

Budapest
2017

1. Introduction

Massive bone defects constitute a major challenge to reconstructive surgery. Autogenous bone grafting is considered the gold standard for filling bone defects even today, despite significant problems arising from donor-site morbidity and limited amount of donor bone (Arrington et al. 1996). Therefore, bone regeneration by means of tissue engineering has attracted increasing interest. The concept of tissue engineering is based on three pillars: (1) scaffolds; (2) cells; and (3) growth factors.

Ceramics are promising materials for tissue engineering because they offer three-dimensional support and serve as a scaffold for cell proliferation, cell differentiation and ultimately for bone formation. A variety of degradable and osteoconductive biomaterials are available and clinically utilized (Petite et al. 2000). Calcium-deficient hydroxyapatite (CDHA) is a member of this high-SSA (high-specific surface area) ceramic group, with a SSA of 20–80 m2/g, approaching the values of about 80 m2/g found in natural bone. Cells adhere more easily to high-SSA ceramics, than to low-SSA (low specific surface area) scaffolds.

To improve their osteogenic potential, scaffolds can be combined with mesenchymal stem cells (MSC) and/or growth factors. MSC are multipotential cells and can differentiate into osteoblasts, chondrocytes, adipocytes, tenocytes. MSC can be isolated from a bone marrow aspirate and rapidly expanded in vitro. Numerous preclinical studies have shown that MSC expanded in vitro can regenerate critical-size bone defects when combined with bone substitutes (Prockop et al. 1997, Petite et al. 2000, Quarto et al. 2001).

Growth factors influence the chemotaxis, differentiation, proliferation and synthetic activity of bone cells, thereby regulating physiological remodeling and fracture healing. Platelet-rich plasma (PRP) contains a number of these growth factors (PDGF, TGF-b1, TGF-b2, IGF, EGF, ECGF) in its natural composition (Kiuru et al. 1991).

Curettage followed by bone cement plugging is a currently accepted surgical treatment of bone tumours that is applied mainly to large cystic lesions, such as giant cell tumours, aneurysmal bone cysts, chondroblastomas, localised in the proximity of the greater joints (Labs et al. 2001). The risk of subchondral cement causing damage to the cartilage and subsequently degenerative arthritis has been cited in the literature, but

remains unproven. Articular degeneration with associated biomechanical changes after treatment with cement has been noted in the weight-bearing area in animal studies, whereas other studies have demonstrated the superior ability of subchondral autogenous bone grafts to restore the subchondral osseus anatomy to its normal state.

2. The aim of the study

The first aim of this retrospective study was to compare and assess the effect of bone grafting and cementing techniques – two common applications used in the treatment of subchondral giant cell tumours of bone (GCTs) – on the development of degenerative changes in the weight-bearing joints of the lower extremity.

To our knowledge, there are sparse data on the effect of PRP on the healing of critical-size long-bone defects. This model, however, is of fundamental interest because it comes close to the situation of non-union where the orthopedic surgeon attempts healing by measures other than simply bone grafting and/or internal stabilization. Therefore, we decided to examine the effect of PRP in combination with autogenous MSC and the aforementioned high-SSA scaffold CDHA in a rabbit model. The main outcome parameters were biomechanical stability, newly formed bone and resorption of the ceramic as shown on micro-computer tomography (micro-CT) and histology.

3. Materials and methods

3.1 Patients and methods

Between 1970 and 2006, 199 patients with giant cell tumours of bone were treated surgically in the Orthopaedic Clinic of Semmelweis University, Budapest, Hungary. The study cohort comprised patients with subchondral GCTs treated by curettage of the proximal femur, distal femur, proximal tibia and distal tibia.

To eliminate factors which can result in secondary osteoarthrosis, 49 patients were excluded from the study for various reasons: pathological fracture, septic complications, local recurrences, non-subchondral localisation or patients with a follow-up of less than 50 months.

When possible, a pneumatic tourniquet was used during the procedure to decrease local bleeding. Extensive curettage was performed. Maximal care was taken to spare the subchondral bone. Bone cement or cancellous bone graft from a bone bank was packed into the cavity of the curetted defect. Post-operative complications were recorded. All patients had a routine follow-up with a physical examination and radiographs of the involved limb every 3 months for 2 years, then every 6 months for 3 years, and then annually thereafter. The radiographs were reviewed and compared with previous images. Patient documentation was reviewed in all cases to monitor signs of degeneration of a given joint over time. The most recent follow-up data were compared with the 24-month and 50-month follow-up data. The area of affected subchondral bone was measured on anteroposterior and lateral radiographs. The subchondral bone was defined as affected when the distance between it and the tumour was less than 3 mm. The GCTs were staged according to the system described by Campanacci: stage 1 lesions were intraosseus, stage 2 lesions were intraosseus lesions with cortical thinning and stage 3 lesions extended extraosseously (Enneking 1987). The size of the subchondral involvement of the tumour was assessed according to the method published by Chen with the percentage of affected subchondral bone calculated as the ratio of the affected length to the total length of the compartment's subchondral bone (Chen et al. 2005).

Degenerative status was defined on the basis of radiological changes, decreased range of motion and pain. Signs of degenerative changes in radiographs were documented.

3.2 Animals

Six- to 9-month-old female New Zealand white rabbits (NZWR) were kept in separate cages, fed a standard diet and allowed to move freely during the study. The following groups (each n=6) were compared: the critical-size defect was filled with: (1) a CDHA scaffold and autogenous MSC; (2) CDHA and PRP; or (3) CDHA, autogenous MSC and PRP. As controls served (4) the CDHA scaffold alone; (5) an empty defect; and (6) a defect filled with autogenous cancellous bone from the iliac crest. Animals were treated in compliance with our institution's guiding principles ‘‘in the care and use of

animals''. The local ethics committee for animal experiments approved the design of the experiment.

3.3 Ceramic scaffolds

Calcium-deficient hydroxyapatite ceramic cylinders of 15 mm length and 4 mm diameter (Robert Mathys Foundation, Switzerland) were produced in an emulsion process (Bohner 2000). The ceramic had a total porosity of 85 vol%, 54 vol% for macropores (0.2–0.6 mm) and 31 vol% for micropores (<5 mm). Its specific surface area approximated 48 m2/g.

3.4 PRP

For the preparation of the PRP, on average 17 ml of blood was obtained from the ear arteries of six anesthetized 6-month old NZWR. The protocol was adapted from Yamada (Yamada et al. 2004). The blood was collected in tubes that were rinsed with heparin and the platelets were counted in chambers. Then, the blood was centrifuged twice: initially at 209xg for 16 min at 20 °C to remove red blood cells and then at 1500xg for 12 min at 20 °C to obtain the platelet pellet. The cell pellet was resuspended in platelet-poor plasma, resulting in an average platelet number of 10.05 $x10^8$/ml. The PRP of the six donors was mixed and stored at -80 °C until needed, and consequently allogenic PRP was used.

3.5 Isolation and cultivation of autogenous rabbit mesenchymal stem cells

Two weeks prior to the surgery when the bone defect was created, bone marrow was harvested from all animals. According to a preoperative randomized protocol animals in the autogenous MSC group (n=6) and the autogenous MSC+PRP group (n=6) received their expanded MSC. The surgical technique was the following: with the animal under general anesthesia, the bone marrow of the tibia was penetrated antegrade via the proximal anterior tibial metaphysis using a sterile bone marrow aspiration needle with a diameter of 3 mm. After reaching the marrow space and removing the trocar, the bone

marrow was aspirated using a 2-ml syringe. The aspirated marrow was mixed in a 15-ml Falcon tube containing 5 ml of pre-digestion medium and 4 ml of Verfaillie medium. Once digestion ceased,10 ml of PBS was added, and the pre-digested marrow aspirate was filtered by use of a 40 μm filter. Subsequently, the cells were counted and afterwards plated in cell culture flasks in modified expansion medium according to Verfaillie. After 24 h, non-adhesive cells were discarded and adhesive cells were washed once with PBS. The medium was changed twice a week. At 80–90% confluence, cells were harvested.

3.6 Loading of cells and application of PRP

All ceramics were incubated overnight at 4 °C in 40-μM/ml fibronectin solution diluted in PBS to improve the adhesion of the cells and because it was found to be beneficial for bone formation (Vogel rt al. 2006). The cells to be transplanted were detached from the culture flasks by trypsin and counted. Five million cells were then resuspended in 3 ml of culture medium and transferred into a 5-ml tube. The ceramics were placed into the medium containing the cells. After 1.5 h of continuous spinning at 37 °C (35x/min), the ceramics were placed into a sixwell plate.

Previous studies demonstrated that loading MSC statically on CDHA had an efficiency of 95%. After loading of the cells the MSC remain in the superficial layers within a depth of 1–2 mm. Forty microliters of freshly thawed PRP was then applied to the ceramics of the PRP group, and subsequently 10 μl thrombin and calcium chloride as added directly before implantation.

3.7 Surgery

The animal model was adapted from Wittbjer et al. as described previously (1982). Briefly, unilateral 15-mm critical-size defects were created in the distal radial diaphysis. The rabbits were anesthetized with an intramuscular injection. A superomedial incision of 3 cm was made over the distal radius, soft tissues were dissected, and the bone was exposed by gentle retraction of the muscles. A 15-mm segmental diaphyseal defect was created with an oscillating saw. The periosteum was removed with the bone and 5 mm of periosteum was stripped from each side of the remaining proximal as well as distal main

fragment. The defect was irrigated with sterile physiological saline solution, and the ceramic (or cancellous bone, or nothing) was press fitted into the defect. Muscles, fascia and skin were separately closed over the defect. Fixation of the osteotomized radius was unnecessary because of the fibro-osseous union of ulna and radius proximal and distal to the surgical site and the press fit of the implant. In the cancellous bone group, the cancellous bone was harvested through a separate 2-cm incision above the posterior iliac crest. The fascia was divided and the edge of the iliac crest was osteotomized. The cancellous bone was then harvested by use of a curette between the layers of cortical bone. The wound was closed in layers. After 16 weeks the animals were killed. After immediate mechanical testing, the specimens were placed in 70% ethanol.

3.8 Biomechanical testing procedure

A four point non-destructive bending test was performed immediately after the animal was killed by means of a testing device adapted from the model of Mattila et al. (1999). First, the forearm was exarticulated at the elbow joint. Then, the wrist and the soft tissues of the forearm were carefully dissected to visualize the area of the bone defect without touching the ceramic or the bone. The ulna was loaded at two points, 40 mm apart from each other. The indentor was positioned at the radius and consisted of two parallel points of identical length that were placed 12 mm apart at each side. The radial defect was centered exactly between these two points. Both the loading points and the indentor were round and had a diameter of 2 mm to avoid cutting into the bone when loaded. The test was motion controlled with a speed of 0.08 mm/s. The data were automatically recorded and stored in a desktop computer interfaced with the material testing device. The strain curves (N/mm) were analyzed for the elastic linear deformation zone with exclusion of the plastic deformation zone. From the slope of the linear elastic deformation curve the stiffness (Young's modulus) was calculated. To account for interindividual differences in bone diameter the stiffness of the operated leg was normalized to the stiffness of the contralateral forearm (in percent). Each contralateral forelimb was measured at the same position as the ipsilateral forelimb.

3.9 Micro-computer tomography

After mechanical testing, the specimens, containing the 1.5-cm segmental defect and 0.5 cm of proximal and 0.5 cm of distal cortical bone adjacent to the defect, were fixed in 70-% alcohol. Each bone block was examined with a micro-computer tomography (micro-CT) system. The microfocus of the X-ray source of the micr-CT system had a spot size of 7 mm and a maximum voltage of 36 kV. The image matrix was 1024 x 1024 pixels. The specimens were placed in a sample holder filled with water. They were oriented in such a way that the long axis of the block was parallel to the axis of the sample holder. A high-resolution protocol (slice thickness 120 mm, feed 60 mm, pixel size 60 mm) was applied. Depending on the length of the specimens, up to 180 slices was scanned perpendicular to the block. To determine the amount of newly formed bone tissue, the best threshold for the CDHA scaffold alone was selected visually followed by determination of the threshold for the CDHA scaffold and newly formed bone together. In addition, the ranges and means of the gray levels characteristic of the CDHA scaffold and newly formed bone were determined. The CDHA scaffold showed a mean gray level of 160±15, while that of the newly formed bonewas 60±15. The visually determined threshold to separate CDHA scaffold from newly formed bone was set at 100, allowing reliable distinction between the two tissue types. Finally, micro-CT slices were compared with the corresponding histological slides to verify the reliability of the discrimination criteria. The digitized data were analyzed with VG Studio Max 1.2.1 software, and the amount of new bone formation (newly formed bone voxels per complete tissue voxels of the initially implanted CDHA volume) was calculated. Resorption was calculated by dividing the voxels of the ceramic that was present after 16 weeks by the voxels of the mean of three CDHA cylinders that were not implanted.

3.10 Histological analysis

After mechanical testing and micro-CT analysis, the non-decalcified specimens were dehydrated in ascending grades of alcohol and embedded in Technovit. During embedding, the positioning of the radius was standardized in an attempt to ensure that the same region was evaluated in all specimens. Then, 50-mm coronal sections with the

radius and ulna parallel were made, using a sawing and grinding. From each animal one section was stained with Goldner's trichrome and one with Giemsa and toluidine. The sections were examined using a light microscope. The Giemsa/toluidine-stained specimens were digitized and analyzed. The type of tissue was identified manually, marked and assigned to a color. In detail, the areas of newly formed bone, connective tissue and ceramic were calculated per total bone defect area. In addition, a 3x4-mm area adjacent to the ceramic/bone interface and, in another approach, the half of the radial defect that was next to the ulna were separately evaluated for area of new bone formation, i.e. the areas of bone per total area were calculated.

3.11 Statistical analysis

Data analysis was performed with SPSS for Windows 15.0 (SPSS Inc., Chicago, IL, USA). Mean values and standard deviations were calculated. The main outcome measures were stiffness during the biomechanical testing and newly formed bone and ceramic resorption in m-CT and histology. These were examined by multifactorial analysis of variance (ANOVA). Differences between the independent variables were checked in post-hoc tests (Tukey's studentized range tests for variables). The extent of bone formation at the interface area and the ulnar half of the bony defect were compared to the extent of bone formation in the total defect area with a matched paired Wilcoxon test. The cumulative arthrosis-free survival time of patients was calculated by the Kaplan-Meier method and evaluated by the Log-Rank test. P values <0.05 were considered significant. All tests were two-tailed.

4. Results

4.1 Clinical Results

Of the 199 patients, 129 had GCTs in the weight-bearing bones of the lower extremity, and 70 in other locations (upper extremity, pelvis, etc.). A subchondral tumour was present in 109 patients (84%). Phenol was used as adjuvant therapy in 85 patients. Seventeen (20%) of the patients treated with phenol showed local recurrence of the tumour, while 16 (36%) of those not treated with phenol showed recurrence.

Eighty patients participated in our retrospective study, with an average follow-up time of 84 months (range: 50– 148 months). The mean age of the patients was 32.4 years (range: 14–69 years). The proximal femur was affected in five patients, distal femur in 45 patients, the proximal tibia in 19 patients and the distal tibia in 11 patients. There were three patients with Stage 1 lesions, 45 patients with Stage 2 lesions and 32 patients with Stage 3 lesions. Average subchondral involvement by the tumour was 27.5% (range: 15–89%) according to the method of Chen et al.

Curettage and bone grafting was performed in 44 patients, while 36 patients underwent cementation after curettage. At the 24-month follow-up, degenerative joint changes were found in six (13.6%) patients of the bone grafting group and in three (8.3%) patients of the bone cemented group. At the 50-month follow-up, seven (15.9%) patients treated with bone grafting and seven (19.4%) patients with cementing showed degenerative signs in the joints, which represents one new patient with degenerative signs among those treated with bone grafting and four new patients with degenerative signs among those treated with cementing. After the first post-operative examination at 24 months, significantly less degenerative changes were found in patients with bone cementing than in those withbone grafting. At the 50-month follow-up and later (range: 50–148 months), however, no significant differences were found between the two groups. These results show that after 24 months there was a significant acceleration of degenerative changes in the cemented group. The initial difference between the two groups equalised over years (Fig. 1.).

The Campanacci staging did not show a significant correlation with degenerative changes at any of the time points in the follow-up ($p>0.05$). However, significant

differences were found between tumour groups involving more or less than 50% of the subchondral bone in the period between 50 and 114 months post-operative ($p<0.05$).4

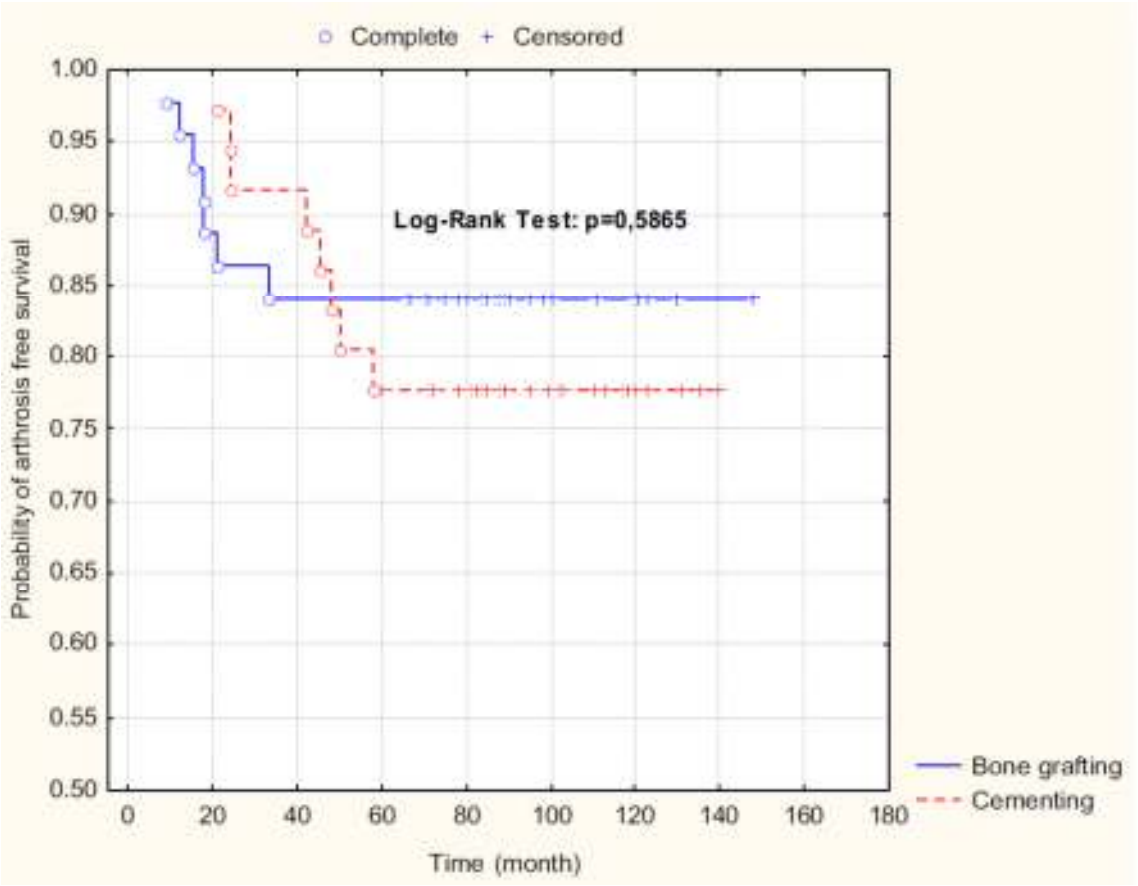

Fig. 1.

Probability of arthrosis-free survival

4.2 Biomechanical results

The relative stiffness of the CDHA, CDHA+MSC, CDHA+PRP and CDHA+MSC+PRP groupswere significantly higher than in the empty group ($p < 0.05$). The autogenous cancellous bone group had significantly higher values than CDHA, CDHA+MSC and CDHA+MSC+PRP ($p < 0.05$), but not than CDHA+PRP. The differences between CDHA, CDHA+MSC, CDHA+PRP and CDHA+MSC+PRP animals were not statistically significant. All operated forearms revealed lower stiffness than the intact contralateral forearms.

4.3. Bone volume and CDHA ceramic resorption measured in micro-CT

The volume of the newly formed bone in the CDHA+MSC, CDHA+PRP and CDHA+MSC+PRP animals was significantly higher than in the animals that received only CDHA ($p<0.05$). Defects treated with autogenous cancellous bone had regenerated entirely. The new bone formation was minimal in the empty control group, which was not significantly different from the CDHA-only group. There were no differences in the volume of the newly formed bone among the CDHA+PRP, CDHA+MSC and CDHA+MSC+PRP groups (Fig. 2.). The residual volume of the CDHA scaffold was significantly lower in the CDHA+MSC, CDHA+PRP and CDHA+MSC+PRP animals than in the CDHA animals ($p<0.05$). There were also no differences in the residual volume of the CDHA scaffold among the CDHA+PRP, CDHA+MSC and CDHA+MSC+PRP groups.

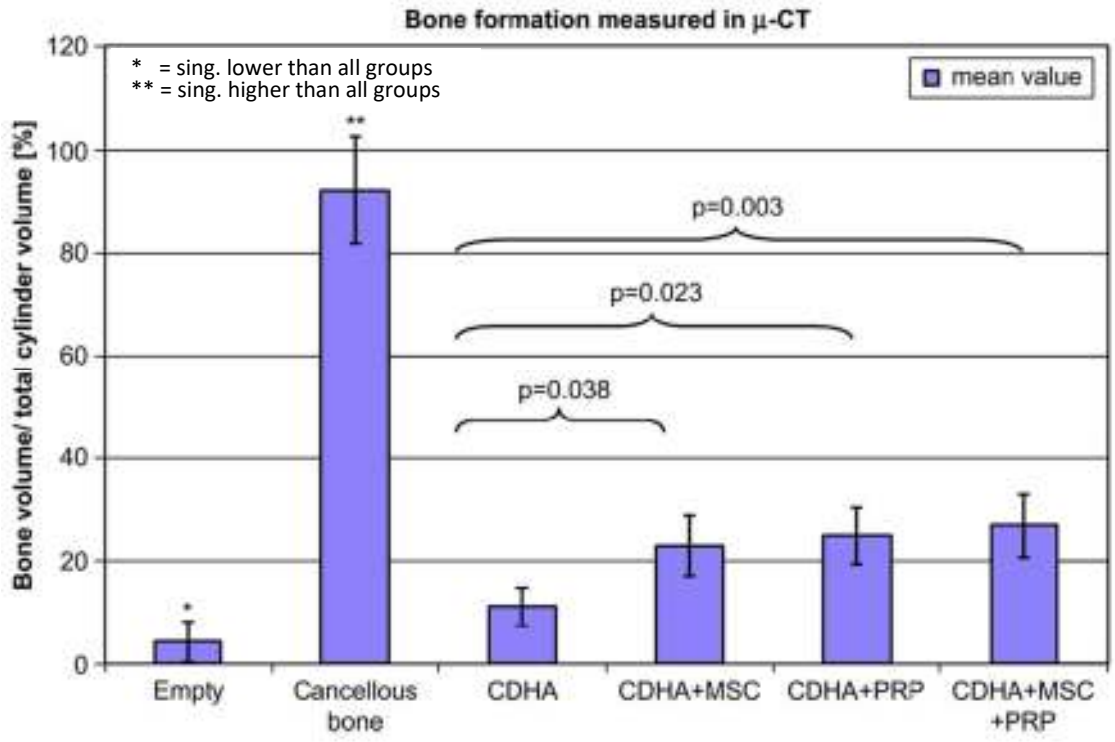

Fig. 2.

The addition of MSC and/or PRP resulted in greater bone formation than in the CDHA-only group. There were no significant differences between the CDHA+MSC, CDHA+PRP and CDHA+PRP+MSC groups. The numbers were n = 4 in the empty group, n = 5 in the CDHA+PRP group and n = 6 in the other groups.

4.4 Histological results

In general, the histological findings were in accordance with the results of micro-CT analysis and the X-rays. Little or no new bone formed in the empty defects. The autogenous bone transplant integrated with the local bone, proximally and distally. The area of newly formed bone was higher in defects treated with CDHA+MSC and with CDHA+MSS+PRP than in defects treated with CDHA alone ($p<0.05$). This trend did not reach significance comparing the empty defect with the CDHA+PRP group.

The ulnar half ($p=0.0005$) and the interface area ($p=0.006$) of the bone defect contained significantly more bone than the total defect surface in the CDHA+MSC, CDHA+PRP and CDHA+MSC+PRP groups. There were no differences between the groups. The bone tissue formed in the periphery of the ceramic pores without a fibrous layer between the bone and the ceramic. This indicates that the scaffold has osteoconductive properties. The pores adjacent to the ulna and in the interface towards the radius were even completely filled with bone.

5. Conclusion

1. After the first post-operative examination at 24 months, significantly less degenerative changes were found in patients with bone cementing than in those with bone grafting. At the 50-month follow-up and later, however, no significant differences were found between the two groups. These results show that after 24 months there was a significant acceleration of degenerative changes in the cemented group. The initial difference between the two groups equalised over years.
2. The results of our study revealed that there was a clear relationship between the size of the subchondral bone involvement and secondary degenerative changes in the joints. Significant differences were found between tumour groups involving more or less than 50% of the subchondral bone in the period between 50 and 114 months.
3. PRP yielded better bone formation than the empty CDHA scaffold as determined by both histology and micro-computer tomography after 16 weeks.
4. No difference was observed between CDHA and CDHA+PRP animals on biomechanical testing.
5. The volume of the newly formed bone in the CDHA+MSC, animals was significantly higher than in the animals that received only CDHA, however, the combination of MSC and PRP did not further improve bone healing. The addition of MSC to PRP could be omitted in the described rabbit model in the future.
6. Furthermore, the resorption of CDHA was improved by the addition of PRP, MSC and MSC/PRP, but there were no differences between the groups. In conclusion, PRP improves bone healing in a diaphyseal rabbit model on CDHA.
7. This study supports the allogenic use of PRP for bone healing as an off-the-shelf therapy.

6. References

Arrington ED, Smith WJ, Chambers HG, Bucknell AL, Davino NA. (1996) Complications of iliac crest bone graft harvesting. Clin Orthop, 329: 300-9.

Bohner, M. (2001) Calcium phosphate emulsions: Possible applications. Key Eng Mater, 192-195: 765-768.

Chen TH, Su YP, Chen WM. (2005) Giant cell tumors of the knee: subchondral bone integrity affects the outcome. Int Orthop, 29: 30-4.

Enneking WF. (1987) Muscoloskeletal tumor surgery. New York, Churchill Livingstone.

Hisatome T, Yasunaga Y, Ikuta Y, Fujimoto Y. (2002) Effects on articular cartilage of subchondral replacement with polymethylmethacrylate and calcium phosphate cement. J Biomed Mater Res, 59: 490-498.

Kasten P, Vogel J, Luginbuhl R, Niemeyer P, Tonak M, Lorenz H, Weiss S, Fellenberg J, Leo A, Simank HG, Richter W. (2005) Ectopic bone formation associated with mesenchymal stem cells in a resorbable calcium deficient hydroxyapatite carrier. Biomaterials, 26: 5879-5889.

Kiuru J, Viinikka L, Myllyla G, Personen K, Perheentupa J. (1991) Cytoskeleton-dependent release of human platelet epidermal growth factor. Life Sci, 49: 1997-2003.

Labs K, Perka C, Schmidt RG. (2001) Treatment of stages 2 and 3 giant-cell tumor. Arch Orthop Trauma Surg, 121: 83-86.

Mattila P, Knuuttila M, Kovanen V, Svanberg M. (1999) Improved bone biomechanical properties in rats after oral xylitol administration. Calcif Tissue Int 64(4): 340-4.

Petite H, Viateau V, Bensaid W, Meunier A, de Pollak C, Bourguignon M. (2000) Tissue-engineered bone regeneration. Nat Biotechnol, 18(9): 959-63.

Prockop DJ. (1997) Marrow stromal cells as stem cells for nonhematopoetic tissues. Science, 276: 71-4.

Quarto R, Mastrogiacomo M, Cancedda R, Kutepov SM, Mukhachev V, Lavroukov A. (2001) Repair of large bone defects with the use of autologous bone marrow stromal cells. N Eng J Med, 344: 385-6.

Vogel JP, Szalay K, Geiger F, Kramer M, Richter W, Kasten P. (2006) Platelet-rich plasma improves expansion of human mesenchymal stem cells and retains differentiation capacity and in vivo bone formation in calcium phosphate ceramics. Platelets, 17(7): 462-9.

Wiltfang J, Kloss FR, Kessler P, Nkenke E, Schultze-Mosgau S, Zimmermann R. (2004) Effects of platelet-rich plasma on bone healing in combination with autogenous bone and bone substitutes in critical-size defects. Clin Oral Implants Res, 15(2): 187-93.

Wittbjer J, Palmer B, Thorngren KG. (1982) Osteogenetic properties of reimplanted decalcified and undecalcified autologous bone in the rabbit radius. Scand J Plast Reconstr Surg, 16(3): 239-44.

Yamada Y, Ueda M, Naiki T, Takahashi M, Hata K, Nagasaka T. (2004) Autogenous injectable bone for regeneration with mesenchymal stem cells and plateletrich plasma: tissue-engineered bone regeneration. Tissue Eng, 10(5-6): 955-64.

Publications related to present thesis

Niemeyer P, **Szalay K,** Luginbühl R, Südkamp NP, Kasten P. (2010) Transplantation of human mesenchymal stem cells in a non-autogenous setting for bone regeneration in a rabbit critical-size defect model. Acta Biomater, 6(3):900-8.
IF:4,824

Kasten P, Vogel J, Geiger F, Niemeyer P, Luginbühl R, **Szalay K**. (2008) The effect of platelet-rich plasma on healing in critical-size long-bone defects. Biomaterials, 29(29):3983-92.
IF:6,646

Geiger F, Lorenz H, Xu W, **Szalay K**, Kasten P, Claes L, Augat P, Richter W. (2007) VEGF producing bone marrow stromal cells (BMSC) enhance vascularization and resorption of a natural coral bone substitute. Bone, 41(4):516-22.
IF:3,966

Szalay K, Antal I, Kiss J, Szendroi M. (2006) Comparison of the degenerative changes in weight-bearing joints following cementing or grafting techniques in giant cell tumour patients: medium-term results. Int Orthop, 30(6):505-9.
IF:0,977

Vogel JP, **Szalay K**, Geiger F, Kramer M, Richter W, Kasten P. (2006) Platelet-rich plasma improves expansion of human mesenchymal stem cells and retains differentiation capacity and in vivo bone formation in calcium phosphate ceramics. Platelets, 17(7):462-9.
IF:1,679

Publications NOT related to present thesis

Antal I, Kiss J, Perlaky T, **Szalay K**, Vancsó P, Oláh Z, Sápi Z, Pápai Z, Szendrői M. (2014) Resection and reconstruction in cases of musculosceletal soft tissue sarcomas. Magy Onkol, 58(1):32-6.

Kiss J, Antal I, Perlaky T, **Szalay K**, Oláh Z, Vancsó P, Révész Z, Rahóty P, Lestár B, Entz L, Szendrői M. (2014) Limb saving surgery in cases of bone sarcomas. Magy Onkol, 58(1):37-46.

Szendrői M, Antal I, Kiss J, Perlaky T**, Szalay K.** (2014) Contemporary management of bone tumors at Semmelweis University. Magy Onkol, 58(2):88-93.

Antal I, Szokoly M, **Szalay K**, Skaliczki G, Szél T, Szendrői M. (2013) Metrimed és Protetim cementezett csípőprotézisek túlélési eredményei 10 évet meghaladó

utánkövetéses vizsgálatunk alapján. Magyar Traumatológia Ortopédia Kézsebészet Plasztikai Sebészet, 56:(4) pp. 273-282.

Holnapy G, **K Szalay**, Szendrői M. (2012) A csípő arthroplasztika tribológiai vonatkozásai. Magyar Traumatológia Ortopédia Kézsebészet Plasztikai Sebészet, 55:(3) pp. 185-194.

Antal I, **Szalay K**, Kiss J, Sápi Z, Szendrői M. (2009) DNS-tartalom és proliferációs index mint az óriássejtes csonttumorok prognosztikus tényezői
Magyar Traumatológia Ortopédia Kézsebészet Plasztikai Sebészet, 52:(2) pp. 139-147.

Skaliczki G, Antal I, Kiss J, **Szalay K**, Skaliczki J, Szendroi M. (2005) Functional outcome and life quality after endoprosthetic reconstruction following malignant tumours around the knee. Int Orthop, 29(3):174-8.
IF:0,676

Skaliczki G, Antal I, Kiss J, **Szalay K**, Szendrői M. (2005) Középtávú életminőség vizsgálat és funkcionális eredmények térdízületi tumor endoprotézis beültetés után. Magyar Traumatológia Ortopédia Kézsebészet Plasztikai Sebészet, 48:(1) pp. 43-51.